HEAT TRANSFER IN PULSATILE FLOW THROUGH SQUARE MICROCHANNELS WITH WAVY WALLS

A THESIS SUBMITTED IN PARTIAL FULFILMENT OF THE REQUIREMENTS FOR THE DEGREE OF

Master of Technology

in

Mechanical Engineering

By

ALOK NARAYAN BEHERA

ROLL NO-213ME3424

DEPARTMENT OF MECHANICAL ENGINEERING

NATIONAL INSTITUTE OF TECHNOLOGY ROURKELA

ROURKELA-769008

JUNE-2015

HEAT TRANSFER IN PULSATILE FLOW THROUGH SQUARE MICROCHANNELS WITH WAVY WALLS

A THESIS SUBMITTED IN PARTIAL FULFILMENT OF THE REQUIREMENTS FOR THE DEGREE OF

Master of Technology

in

Mechanical Engineering

By

ALOK NARAYAN BEHERA

ROLL NO-213ME3424

Under the guidance of

Dr. MANOJ KUMAR MOHARANA

DEPARTMENT OF MECHANICAL ENGINEERING

NATIONAL INSTITUTE OF TECHNOLOGY ROURKELA

ROURKELA-769008

JUNE-2015

NATIONAL INSTITUTE OF TECHNOLOGY ROURKELA

CERTIFICATE

This is to certify that the thesis entitled, "**HEAT TRANSFER IN PULSATILE FLOW THROUGH SQUARE MICROCHANNELS WITH WAVY WALLS**" submitted by Mr. Alok Narayan Behera in partial fulfilment of the requirement for the award of Master of Technology Degree in Mechanical Engineering with specialization in Thermal Engineering at National Institute of Technology, Rourkela (Deemed University) is an authentic work carried out by him under my supervision and guidance.

To the best of my knowledge, the matter embodied in the thesis has not been submitted to any other University/ Institute for the award of any degree or diploma.

Date 01-06-2015

Dr. Manoj Kumar Moharana
Assistant Professor
Department of Mechanical Engineering
National Institute of Technology Rourkela
Rourkela– 769008

SELF DECLARATION

I, Mr Alok Narayan Behera, Roll No. 213ME3424, student of M. Tech (2013-15), Thermal Engineering at Department of Mechanical Engineering, National Institute of Technology Rourkela do hereby declare that I have not adopted any kind of unfair means and carried out the research work reported in this thesis work ethically to the best of my knowledge. If adoption of any kind of unfair means is found in this thesis work at a later stage, then appropriate action can be taken against me including withdrawal of this thesis work.

Date 01-06-2015
Place NIT Rourkela

Alok Narayan Behera
Alok Narayan Behera

ACKNOWLEDGEMENT

It is my privilege to express my deep sense of gratitude and sincere thanks to **Dr. Manoj Kumar Moharana** (Assistant Professor, Department of Mechanical Engineering), for his valuable guidance and encouragement for progress my project title "HEAT TRANSFER IN PULSATILE FLOW THROUGH SQUARE MICROCHANNELS WITH WAVY WALLS". Working under his guidance is an excellent learning experience that I will cherish for a long time.

I am also thankful very much to my classmates who help in completion of my project work.

Date 01-06-2015
Place NIT Rourkela

Alok Narayan Behera
Alok Narayan Behera

ABSTRACT

A three-dimensional numerical analysis is performed to understand the effect of axial wall conduction on conjugate heat transfer during single phase pulsatile flow in a square microchannel with wavy walls (wall faces are parallel to each other). A microchannel of inner width and height are 0.4 × 0.4 mm^2 and length of 30 mm is considered for the numerical simulation. The wavelength and amplitude of the vertical wavy shaped channel wall are 12 mm and 0.2 mm respectively. The working fluid is taken as water which enters the channel at 300 K temperature and constant heat flux boundary condition is imposed on the entire bottom surface of the microchannel. All the remaining walls of the microchannel exposed to surrounding are kept insulated. The velocity at the inlet of channel is the combination of a fixed component of velocity and fluctuating component of velocity which varies sinusoidally, thus causing pulsatile velocity at the inlet (amplitude, A = 0.2) with variation of frequency from 2 Hz to 10 Hz. Simulations has been performed for constant flow Reynolds number (Re = 100) and wall thickness to inner radius ratio (δ_{sf} = 1) with varrying solid wall to fluid conductivity ratio (k_{sf} from 0.344 to 715). It is observed that k_{sf} play a key role to enhance heat transfer due to axial wall conduction. Change of pulsation frequency corresponds to Womersley number (Wo = 1.414, 2, 245, and 3.163) does not affect local Nu. From the numerical simulation, it is obtained that overall Nusselt number function of Re and thickness ratio (δ_{sf}) at particular Wo. Overall Nusselt number increases with k_{sf} up to an optimum value then decreases due to the effect of axial wall conduction.

Keywords: pulsatile flow, microchannel, axial wall conduction, Womersley number, conjugate heat transfer.

Contents

List of figure

List of Table

Nomenclature

A	Amplitude of pulsation
C_p	Specific heat at constant pressure, J/kg-K
D_h	Hydraulic diameter of the channel, mm
f	Frequency of pulsation, Hz
h(z,t)	Instantaneous local heat transfer coefficient, W/m^2-K
k_s	Thermal conductivity of substrate wall, W/m-K
k_f	Thermal conductivity of working fluid, W/m-K
k_{sf}	Ratio of k_s and k_f
L	Length of the tube, m
L_c	Characteristic length (L_c = D), mm
M	Axial conduction number
Nu_{avg}	Overall Nusselt number
Nu(t)	Space average instantaneous Nusselt number
Nu(z)	Time average local Nusselt number
Nu(z,t)	Instantaneous local Nusselt number
P	Gauge pressure, N/m^2
Pe	Peclet number
Po	Poiseuille number
Pr	Prandtl number ($\mu c_p/k_f$)
Re	Reynold's number ($\rho U D_h/\mu$)
$\overline{q'}$	Heat flux experienced at the solid-fluid interface, W/m^2
q'	Wall heat flux applied at the bottom of solid substrate
q_z	Local heat flux experienced along the axial direction of the channel, W/m^2

St	Strouhal number
T	Temperature, K
t	Time, s
U	Average velocity at the channel inlet, m/s
Wo	Womersley number ($L_c(\omega/\nu)^{0.5}$)
X	Axial coordinate

Greek Symbol

ν	Kinematic viscosity, m^2/s
ρ	Density, kg/m^3
δ_f	Inner radius of the tube, mm
δ_s	Thickness of the tube wall, mm
δ_{sf}	Ratio of δ_s and δ_f
μ	Dynamic viscosity, kg/m-s
ϕ	Non-dimensional heat flux
Θ	Non-dimensional temperature
ω	Angular frequency, rad/s
θ	Time period, s
∇	Differential operator
Φ	Viscous dissipation function

Subscript

f	Fluid
fi	Fluid inlet
fo	Fluid outlet
w	Channel wall
in	Inlet
out	Outlet
av	Average
r	Relative
s	Steady state
t	Transient/unsteady state
*	Non-dimensional quantity
q	Constant heat flux boundary condition

Chapter-1

Introduction

As per modern days all electronic equipment such as microchip inside the computer, laptop, television, etc. need higher cooling rates. As per conventional laws of heat conduction, the rate of heat transfer directly depends on the temperature difference, surface area and also depends on the turbulence created inside the channel. It is not always possible to increase temperature difference, so it is better to use microtube/microchannel that improve the rate of cooling. Microtubes/microchannels have higher surface area per unit volume than the conventional channels, so these are used in many cases for cooling processes. Also by using the wavy microchannel, the turbulence is achieved which also improves the rate of cooling. By the development of micromachining, the requirement and application in the field of heat transfer and fluid flow is day by day increasing. Some of the applications of micromachining in heat transfer and fluid flow are found in Khandekar and Moharana [1]. It is easier to manufacture different size and shape of the microchannel. So microchannel/microtube are gaining much more importance in engineering applications. Generally the microchannel thickness is more compared to the inside radius of the channel which shows axial back conduction effect. This effect also depends on the physical properties of the material, working fluid and flow condition. There are so many types of flow apart from uniform (steady) flow in engineering application. In most of these cases, the flow is oscillating.

1.1 Pulsatile flow

There are many literatures on fluid flow and heat transfer whose focus is on steady flow through conventional as well as microtube/microchannel for single phase and two phase system. Apart from steady flow there also exist two types of flow in engineering applications. There are (i) oscillating flow and (ii) pulsatile flow. Oscillating flow is flow in which fluid swings back and forth about one fixed point with a frequency, when the oscillating flow is restricted in one particular direction, the flow is known as pulsating flow. Pulsating flow is varying transitionally in one direction. Pulsatile flow is mainly characterised by 2 parameters as follows (i) pulsating frequency or Womersley number (Wo) and (ii) amplitude of oscillation. Effect of pulsating inlet and waviness of the channel plays an important role in heat transfer that is a very interesting problem for a researcher due to their many applications in today's life.

1.2 Applications of pulsatile flow

Pulsatile flow has many applications in all fields, but the majority of them are in the biological field. Exchange of air within the body (respiratory system) and blood circulation (cardiovascular system) are the application of pulsatile flow in human body. There are two types of vessels present within the human body i.e. artery and vein. The blood circulation is taking place through the cardiovascular system, called heart that consists of four chambers from which oxygenated blood is carried by arteries. The arteries distribute blood in all parts of the body. Similarly, veins collect deoxygenated blood from the whole body and transfer it to the heart. Blood circulation is completely controlled by valve mechanisms i.e. opening and shutting of valves at particular time intervals leading to a pulsatile flow of blood.

The respiratory system consists of the nostril, larynx muscle and lungs. The major function of the nostril is to take air from the outside atmosphere. The air then goes to the larynx and then to trachea that is further divided into two parts namely bronchi, which is connected to each of the lungs to transfer air. Respiration in human means intake of oxygen from the outside

atmosphere and exhaling carbon dioxide to the outside atmosphere. The major processes in respiration are breath-in or inhalation and breath-out or exhalation. In the respiratory system, the diaphragm acts as piston similar to IC engine. At the time of breath, the diaphragm moves downward creating a vacuum so that air enters into the lungs. Then in breath out the operation, the diaphragm moves in opposite direction. As a result, air is removed out from the lungs to the outside atmosphere. Here due to the upward and downward moment of the diaphragm a periodic pulsatile motion of air is created.

There are many other engineering applications of pulsatile flow such as reciprocating engine, IC engine, pulse combustor, ramjet, pulsating heat pipe, etc. In case of pulse combustor, the combustion of solid, liquid and gaseous fuel takes place periodically. It basically consists of an inlet valve, a combustion chamber and a resonance tube for exhausting gases. The air and fuel enter into the combustion chamber through the valves, which is then ignited with the help of a spark plug. The combustion increases the pressure of the gases results closing of valves and gases moves towards the exhaust. Due to this vacuum created in the combustion chamber, it results in the opening of valves and allows fuel-air for combustion that are ignited by the hot environment. Furthermore, some exhaust gases flow back to the combustion chamber without the help of spark plug. The combustion process takes place repeatedly by periodic variation of air and fuel flow.

There are many practical engineering applications involving severe vibration in which oscillatory motion of working fluid moves in a forward direction. In particular cases, the flow is not continuous but oscillating due to the presence of barriers or obstacles present on the path of flow or complex shapes of devices. We could see in our practical life examples of these types of pulsating flow such as flow in penstock of a hydraulic power plant that is achieved by closing the valve (surging). In addition, cavitation in pipes is also an example of this type of fluid flow.

1.3 Motivation of present work

As per the above discussion, we see that there are many thermal and biological applications which are affected by the pulsatile flow. Due to flow pulsation, the convection heat transfer rate increases. The effect of pulsation in the wavy microchannel is a challenging problem for researchers because there are many applications that have pulsatile fluid flow in the conventional channel as well as in microchannel. In the next chapter, the detailed literature review of pulsatile flow and its effect on heat transfer are discussed. There are many literatures on pulsatile flow in micro and mini-channel in addition to the wavy channel, but flow through the wavy channel and conjugate heat transfer effects were not considered till now. The motivation to start the work is to fill this literature gap. By seeing huge application of pulsatile flow in thermal as well as in biological field, a study must be needed to find out the effect of pulsatile flow in conjugate heat transfer which increase the efficiency for better design of thermal equipments.

Chapter-2

Literature review

There are much literatures available on experimental, numerical and analytical study of thermo- hydrodynamics of single phase steady and pulsating flow in pipes, straight channel, and corrugated channel. Hence all the literature review divided into two category:

- Flow through straight channel
- Concept of microchannel and axial back conduction
- Flow through corrugated channel

2.1 Flow through straight channel

Uchida [2] studied the pulsating flow on steady laminar motion of fluid through a pipe of circular cross section. Due to pulsatile flow, velocity magnitude is maximum towads the wall instead of centre line of the pipe. He was also obtained the velocity profile for pulsatile flow in pipe. The phase lag increases with frequency. Further in [2, 3] different researcher work on pulsatile flow and obtained the annular effect, phase lag, and periodic axial fluctuations of temperature in pipe subjected to pulsating inlet.

Amir and Nourah [3] developed a correlation for heat transfer coefficient in steady and pulsatile flow of air through a rigid circular pipe. A critical value of 2.1×10^5 for dimensionless number was taken. It was found that when $Re < 2.1 \times 10^5$ no improvement in Nu, but when $Re > 2.1 \times 10^5$ Nu enhanced significantly.

Siegel and Perlmutter [4] studied heat transfer for pulsating laminar flow through duct. They considered parallel plates having uniform wall temperature and constant wall heat flux

separately. The flow through pipe was laminar and pulsatile. For uniform wall temperature condition, they were found that Nu show periodic axial fluctuation.

Faghri et al. [5] analytically studied on heat transfer of pipe with laminar pulsating inlet. They found that temperature field divided into the steady mean part and harmonic part due to the velocity pulsation. They obtained that due to the interaction between velocity and temperature oscillation creates an extra term for the enhancement of heat transfer.

Karmercan and Gaine [6] studied the pulsation effect on heat transfer in double pipe heat exchange through which water stem used as working fluid experimentally. They considered five different displacement amplitude for each flow rate where the flow pulsation frequency vary up to 300 cycle/minute. It was found that highest enhancement of heat transfer coefficient observed at transition flow and heat transfer increase with increase in pulsation.

Cho and Hyun [7] studied pulsating flow and heat transfer in a pipe numerically. They solved numerically for a wide range of frequency and amplitude. They found that Nu may be increase or decrease as per the change of frequency and deviation of Nu was very small compared to a steady flow.

Kim et al. [8] numerically studied thermally developed region of pulsating channel flow with uniform temperature wall condition. The simulation carried out for Pr = 0.7, Re = 50, for different amplitude (A) and dimensionless pulsation frequency (M).From this they obtained that for low value of M velocity profile same for both steady and pulsatile flow but in case of large M profile narrow at wall due to flow pulsation. The effect of pulsation on Nu was more in entrance region and very less in fully developed region. Pressure gradient increases with pulsation frequency.

Moschandreou and Zamir [9] studied analytically the effect of flow pulsation in the pipe with uniform heat flux boundary condition. They observed that for the moderate value of

frequency lead to increase the bulk mean temperature of fluid and heat transfer. They also showed peaks were higher at low Pr.

Hemida et al. [10] studied heat transfer in laminar pulsating flow through pipe subjected to uniform wall heat flux. They solved this by both analytically and numerically. The result showed a contradiction to Moschandreou and Zamir [10] i.e. they obtained that heat transfer decrease by using pulsating flow.

Yu et al. [11] analytically studied pulsating laminar flow in a circular tube of constant heat flux. They observed that temperature contour and Nu fluctuate due to pulsation and depend on different parameters such as frequency, amplitude, and Pr. They also conclude that flow pulsation did not affect the time average Nu.

Chattopadhyay et al. [12] studied pulsatile flow in a circular pipe subjected to uniform wall temperature numerically by the SIMPLE algorithm with momentum interpolation technique. They did the simulation for a wide range of amplitude (0 - 1.0) and frequency (0 – 20 Hz).They found that time averaged-Nu not affected by flow pulsation, but Nu fluctuate with time inside the developing region.

Mehta and Khandekar [13] numerically studied the effect of flow pulsation in two type of flow domain (i) flow through axisymmetric circular pipe and (ii) flow through parallel plates in which flow pulsation in transverse direction. They simulated results by using CFD commercial software FLUENT 6.3. They studied the effect of Reynolds number (Re), Prandtl number (Pr), amplitude ratio (A) and pulsation frequency (Womersley number, Wo) on time-averaged and instantaneous heat transfer and friction factor (Po).They observed that Nu did not vary in fully developed region due to flow pulsation compare with steady flow. Effect Re,A and frequency of pulsation (Wo) were not appreciable for Nu enhancement but Pr play crucial role in case of heat transfer i.e. Pr value inversely proportional to time-averaged relative Nu. They obtained in case (i) or axial flow pulsation no enhancement of heat transfer but in case

(ii) or transverse flow pulsation enhancement of time-averaged Nu in developing region for larger frequency (Wo) and smaller spacing ratio.

Persoons et al. [14] experimentally studied the effect pulsatile and steady flow in a microchannel heat sink. To get the flow pulsation they used pulsating flow generator which adjust the pulsatile flow by changing amplitude and frequency. They did the experiment for different range of parameters steady, pulsating Re and Womersley number in a single microchannel. They found that heat transfer enhanced in case of pulsatile flow as compared with steady flow i.e. enhancement factor up to 40% with respect to steady flow. They observe that for small pulsation amplitude (Re_p / Re < 0.2) the heat transfer enhancement is negligible or less compared to steady flow but for large pulsation amplitude (Re_p / Re > 0.2) heat transfer enhancement with an increase in (Re_p / Re).

Kumar and Agrawal [15] experimentally studied microchannel blood flow over a range of hydraulic diameter from 70 to 1000 μm. The set up consist of pressure gauge, microchannel and peristaltic pump which create pulsatile flow in the blood. They measured blood viscosity by Contraves Low Shear 30 viscometer. They reported the variation of flow rate vs. pressure drop and relative viscosity vs. strain rate for circular and trapezoidal microchannel. They found that pressure drop increases with flow rate for all type of microchannels. Relative viscosity increases with strain rate for circular cross section channels and decreases for trapezoidal cross-section channels.

2.2 Concept of microchannel and axial wall conduction

The microchannel is defined as the dimensions less than 1 mm and greater than 1 micron. In case of conventional channel, the wall thickness is very less compared to inner radius but in case of microchannel the wall thickness is equal or more than the inner radius of the channel. Due to having more surface area to volume ratio microchannel lead to enhancing heat transfer more than the conventional channel. Micro heat exchanger plays an important role in thermal

engineering applications. Axial back conduction plays an important role in case of micro heat exchanger which was not a new concept. It was also found in conventional channel but magnitude is negligible quantity due to less wall thickness in comparison of inner radius.

Maranzana et al. [16] studied both analytically and numerically to visualize the effect of axial wall heat conduction in mini/microchannel. They introduced a dimensionless number which signifies axial wall conduction known as 'axial conduction number (M)'. M defined as:

$$M = \frac{q'_{conductive}}{q'_{convective}} = k_s \frac{(\delta_s.\omega)/L}{(\rho.C_p.\delta_f.\omega.U_{av})} \quad (1)$$

They concluded that when $M < 10^{-2}$ axial conduction is neglected in the micro channel. M usually very low in case of macro channel because of low solid to fluid thickness ratio (δ_{sf}). They did the analysis based on assumption that the temperature difference between inlet and outlet of solid substrate (ΔT_s) and fluid domain (ΔT_f) in the axial direction are same. But the above assumption is not write in all case.

To avoid the limitation in Maranzana et al. [16], Zhang et al. [17] numerically studied the effect of axial back conduction in thick circular microtube, outer wall subjected to uniform wall temperature. They consider both ΔT_s and ΔT_f effect. They found that solid to fluid conductivity ratio (k_{sf}) plays a vital role in case of heat transfer. They obtained maximum value of Nu was about 4.3. They conclude that axial heat conduction depend on several parameters like solid to fluid conductivity ratio (k_{sf}), solid to fluid thickness ratio (δ_{sf}), Reynolds number (Re) and Prandtl number (Pr).

Cole and Cetin [18] analytically and numerically studied the effect of axial conduction of heat transfer in parallel plate micro channel subjected to uniform wall heat flux boundary condition. The analytic solution is in integral form by Green's function and numerical results for different flow velocities (Re), wall thickness, heating length and wall conductivity by quadrature. They concluded that axial wall conduction is more in following case (i) lager wall

thickness to channel height ratio (ii) small Peclet number (iii) small length over height ratio of microchannel and (iv) thermal conductivity of solid wall is more than the thermal working fluid conductivity. The axial wall conduction is negligible for lower thermal conductivity of solid wall and high Peclet number (Pe > 100).

Moharana et al. [19] experimentally and numerically studied axial conduction performance of hydrodynamically and thermally developing single phase flow in rectangular minichannel array subjected to constant wall heat flux at the bottom of substrate wall while other surface are adiabatic. They did the experiment by using stripe heater for heating purpose. They fixed certain parameters like Re varied from 150 to 2500 and Prandtl number varied between 3 and 4. They found that laminar flow becomes turbulent after Re $\approx$ 1100 i.e. it was the transition region. In entire experiment, Po and local Nu are function of Re. They found that higher value of axial conduction number (M) lead axial wall conduction. The variation of Nu along axial direction affected by parameter M i.e. higher M lead to low Nu. They conclude that low conductivity solid wall material reduce axial wall conduction effect.

Moharana and Khandekar [20] numerically studied axial back condition in microtube subjected to both uniform wall temperature and constant wall heat flux applied on outer surface of micro tube and side wall of tube are adiabatic. They took 2D axisymmetric geometry for simulation to minimize the calculation time. Wide range of flow rate (Re), conductivity ratio (k_{sf}) and tube wall thickness to inner radius ratio (δ_{sf}) for simulation. The reported that k_{sf} play an important role in role of axial back conduction. They plotted the graph nondimensional bulk mean temperature and tube wall temperature and found that for higher k_{sf} the constant wall heat flux boundary condition look like constant wall temperature due to severe axial back conduction. They also found an optimum k_{sf} value for which average Nu is maximum in case of constant heat flux boundary condition, but it is not found in case of constant wall temperature boundary condition. In case of constant heat flux average Nu increases up to an

optimum value then decrees with an increase in k_{sf}, but in case of constant wall temperature average Nu decreases with increase in k_{sf}. In both cases, higher δ_{sf} leads to higher axial back conduction.

Moharana et al. [21] studied heat transfer in square microchannel subjected to constant wall heat flux at bottom of solid substrate while other surfaces are adiabatic. They carried out the numerical simulation for large range of channel wall to fluid thickness ratio (δ_{sf}), channel wall to fluid conductivity ratio (k_{sf}) and flow rate (Re). They concluded that conductivity ratio k_{sf} play key role in axial wall conduction as Moharana and Khandekar [20]. Larger k_{sf} value leads to decrease average Nu due to severe axial back conduction and small value of k_{sf} lead to a channel of zero wall thickness subjected to constant wall heat flux applied to one side of substrate and remaining are adiabatic. They also reported that for constant Re and δ_{sf} there exist an optimum k_{sf} where the value of average Nu is maximum. They also show the variation of dimension less flux, wall temperature and bulk fluid temperature in axial direction for different Re and δ_{sf}. They also reported that δ_{sf} is proportional with axial back conduction due to increase in thermal resistance.

Moharana and Khandekar [22] numerically studied the axial back conduction effect due to changing aspect ratio of the rectangular microchannel. They took solid substrate of size ($0.6\times0.4\times60$ mm^3) while channel height and width are variable i.e. aspect ratio (width/height) vary from 0.45 to 0.4.They fixed the Re = 100 and Pr = 5.85 for a wide range of k_{sf} from 12.2 to 635 for simulation. In this case Re value is low because it leads axial back conduction [6]. Channel subjected to constant heat flux at the bottom of the substrate wall, and others are kept insulated. They vary aspect ratio in four different way keep constant (i) area of channel cross section (ii) heating perimeter (iii) channel width and (iv) channel height. They also found an optimum Nusselt number as [20, 21]. They reported that for a particular k_{sf} value of Nu is minimum at aspect ratio nearly equal to 2. They also found that the decrease in channel aspect

ratio beyond the minimum value or increasing channel height for fixed channel width, results decrease of the effective thermal resistance, results an increase in average Nusselt number. They found that it was difficult to manufacture low aspect ratio microchannel.

Yadav et al. [23] numerically studied axial conduction as per Moharana and Khandekar [20], but they use Helium as working fluid instead of water keeping other condition same. They took a micro tube of inner diameter 0.4 mm and length of 60 mm subjected to 100 K at the inlet of the tube for simulation. They considered varying flow (Re), conductivity ratio (k_{sf}) and tube wall thickness to inner radius ratio (δ_{sf}). They obtained optimum k_{sf} as per [20, 21, and 22] where average Nu is maximum. They also concluded that for higher wall thickness (δ_{sf}) average Nu is low and the average Nu increases with Helium flow rate.

Mishra and Moharana [24] numerically studied axial conduction of pulsatile flow through microtube subjected to sinusodially varying pulsatile flow velocity at inlet and other boundary conditions same as [5,8]. They carried out the simulation for wide range of conductivity ratio (k_{sf}) and frequency of pulsation (Womersley number Wo) keeping thickness ratio (δ_{sf}), flow rate (Re) and amplitude (A) as constant. They reported that there exist an optimum value of k_{sf} for particular Wo same as [20, 21, 22, 23] where steady flow in microtube and microchannel. Heat transfer is very less in case of pulsation frequency. Average Nu is maximum at optimum k_{sf} and decreases by increasing kbeyond optimum value similar to Moharana et al. [21].They reported that lower k_{sf} leads to increase heat transfer. They reported that by changing phase angle from 0 to 90, results decrease in fluid and wall temperature and increase in dimensionless heat flux. They obtained that effect of Wo is more inside the developing region and by increasing Wo the value of time average relative Nu increases for all k_{sf} in axial direction and the values are less than one indicate heat transfer less compared to steady state.

2.3 Flow through corrugated channel

Sawyers et al. [25] studied both numerically and analytically in the 3-D corrugated microchannel. Reynolds number range up to 250 to avoid turbulence. From this, it was found that heat transfer higher in case of wavy channel than flat plate due recirculation zone. When the flow is stronger in the transverse direction, the recirculation zone destroyed and decrease heat transfer.

Islamoglu and Parmaksizoglu [26] were studied experimentally the effect of channel height on the enhancement of heat transfer in the corrugated heat exchanger channel. In this case, the channel height is 5 and 10 mm, corrugation angle 20^{o} and flow range $1200 \leq Re \leq 4000$.By increasing the height of the channel both Nusselt number and friction factor increases and goodness, factor decreases slightly.

Naphon [27] was studied the effect of wavy geometry configuration on temperature and flow distribution. In this study, the finite volume method with the structured uniform grid is used to solve turbulence problem. Effect of heat transfer studied for different wavy geometry under constant wall heat flux boundary condition. In result, it was found that the sharp edge results a significant increase in heat transfer. So wavy plate use in a heat exchanger to improve thermal performance.

Sui et al. [28] studied numerically in CFD software package heat transfer and fluid flow in a wavy microchannel by dynamic system technique (Poincare section) is analyzed the fluid mixing. They found when liquid flow through wavy channel leads to create secondary flow (Dean Vortices) which leads to chaotic convection greatly enhance heat transfer coefficient with little pressure drop penalty. By increasing waviness, the heat transfer also increases.

Abeb and Ahmed [29] were studied laminar forced convection heat transfer and fluid flow characteristics in a corrugated channel numerically. Here constant wall temperature boundary condition is superimposed. Governing equations in 2-D Cartesian coordinate solved by finite

difference method (Body Fitted Coordinate system). From this, it was found that by increasing wavy angle at particular Reynolds number heat transfer and pressure drop increases.

Mohammed et al. [30] numerically studied heat transfer enhancement in wavy microchannel heat sink. In this water flow through wavy microchannel of different amplitude are studied where range of 100 to 1000 flow. The 3-dimensional governing equations solved by finite volume method (FVM). From this they found that heat transfer performance better than the same cross-sectioned straight channel, pressure drop penalty was very small, friction factor and wall shear stress increase with the amplitude of wavy channel.

Sui et al. [31] experimentally studied heat transfer and friction flow in a wavy microchannel having a rectangular cross section. Here they were considered wavy channel of fixed width of 205 μm, depth of 404 μm, the wavelength of 2.5 mm and waves were parallel. Experimental result of this compared with a straight channel of the same cross section and length found that heat transfer enhance in case of wavy channel that was more than the straight channel.

Gong et al. [32] studied flow and heat transfer in a microchannel with wavy wall numerically using CFD solver, FLUENT. Here they take 3D wavy channel by varying the amplitude, wavelength and aspect ratio for different Re between 50 and 150 with constant wall heat flux 47 W/cm^2. They took two type of wavy channel i.e. crests and troughs facing each other alternatively by phase angle 180^o (serpentine channel) and crests and troughs facing each other (raccoon channel). It was found that in both the cases the heat transfer more than straight channel but in case of serpentine channel improvement up to 55% more that of microchannel with straight walls.

Sui et al. [33] numerically studied fluid flow and heat transfer through wavy channel with rectangular cross section using CFD software package. From this, they found Dean vortices or secondary flow when liquid flow through the channel leads to convective mixing of fluid which enhance heat transfer. Transition flow is getting by increasing Re due to complex shaped Dean

vortices formed flow direction. All numerical simulation carried out with uniform wall temperature and water flow through it result in heat transfer performance better than that of the straight channel of the same cross section with small pressure drop penalty.

Nikhil and Shailendra [34] experimentally studied heat transfer analysis of corrugated heat exchanger of different plate geometry. The corrugated shape of plate heat exchanger leads to turbulence due to the larger heat transfer surface area. An experiment carried out for different chevron angle, Re, Prandtl number. From this experimental data correlation estimated Nusselt number function of Re, Prandtl number, and chevron angle.

Yin et al. [35] numerically studied the effect of phase shift of wavy channel to show flow and heat transfer characteristics. They considered sinusoidal wavy channel of different phase shift between the upper and lower plate having the same diameter and constant wall temperature. From this, it was found that Nu increases with increasing Re because of increasing rate of heat transfer and Nu decreases with increasing phase shift due to a decrease of recirculation. All Nu values were large than the straight channel. In all channel, goodness factor decreases inversely with Re. The optimal thermal performance was obtained for 0^o phase shift channel.

Ozbolat et al. [36] studied heat transfer and flow characteristics in 2D corrugated channel using finite volume method based on SIMPLE technique. Sinusoidal wavy channel having constant wall temperature of the wall were specified. Here two type of corrugated channel were taken first wavy channel and second one rectangular corrugated channel. From this corrugated channel was always more heat transfer than the straight channel and by increasing Re the isothermal lines move toward the corrugated wall and Nu increase.

Pehlivan et al. [37] experimentally studied forced convection heat transfer in different shape corrugated channel. They considered different types of the corrugated channel for analysis with constant wall heat flux of 616 w/m^2 varying Re 1500 to 8000.Nu,convective heat

transfer coefficient(h),Colburn factor(j) and enhancement ratio (E) were studied against Re. From this, they found by increasing corrugated angle lead to increasing rate of heat transfer.

Nandi and Chattopadhay [38] numerical study of developing flow in wavy microchannels (serpentine channel) under pulsating flow inlet. Here they took 2D wavy microchannel with constant wall temperature boundary condition and sinusoidal varying velocity at the inlet. The unsteady solution of 2D Navier-Strokes equation was obtained by using SIMPLE algorithm with the momentum interpolation technique. From the simulation they found that heat transfer performance is more better in case of pulsatile inlet than that of steady flow in microchannel at different amplitude (0.2, 0.5, 0.8) and frequency (1, 5 & 10).

Nandi and Chattopadhay [39] numerical investigation of developing flow and heat transfer in raccoon type microchannels under inlet pulsation. As per the above thesis all the result were same i.e. heat transfer performance was better in case of pulsatile flow than steady for different amplitude (0.2, 0.5, 0.8) and frequency (1, 5, 10) but only change that the wavy channel was raccoon type instead of serpentine channel.

Above literatures shows contradictory results regarding the pulsation flow through channel. Very first question is that pulsatile flow increase or decrease heat transfer from steady state case? But from the above literature it is very difficult to say, because of diverging conclusion such that (i) pulsation increase heat transfer[5, 6] (ii) decrease heat transfer[10] (iii) no effect on heat transfer[4, 11, 12, 13] (iv) either increase or decrease heat transfer depend on parameters[7, 8, 9]. Secondly the channel corrugation also enhance heat transfer [25 - 39]. There are no literature that deals with the study of axial wall conduction or conjugate heat transfer in pulsatile flow wavy microchannel.

Chapter-3

Numerical simulation

3.1 Problem formulation

A parallel wavy wall microchannel having height of fluid (δ_f), thickness of solid substrate below fluid (δ_s), side wall thickness(ω_s) and length (L) is shown in the following diagram. In this case, water is used as working or flowing fluid in microchannel having inlet temperature at 300K and Pr=7. The pulsatile velocity varies sinusoidally with time leading to the development of pulsatile flow in the channel. The pulsatile velocity inlet (U_{in}) is having two components, one is fixed component (U_{av}), and the other is fluctuating component (U_{av}.A.sin (ωt)) that sinusoidally vary with time. The width (ω_f) and height of fluid (δ_f) in the fluid channel are constant at 0.4 mm, and the length of the channel (L) is 30 mm. So the hydraulic diameter (D_h) is 0.4 mm. The side view and front view of the computational domain is also shown in the diagram. The sinusoidal curve of pulsatile flow is shown below where the phase angles are indicated in degrees.

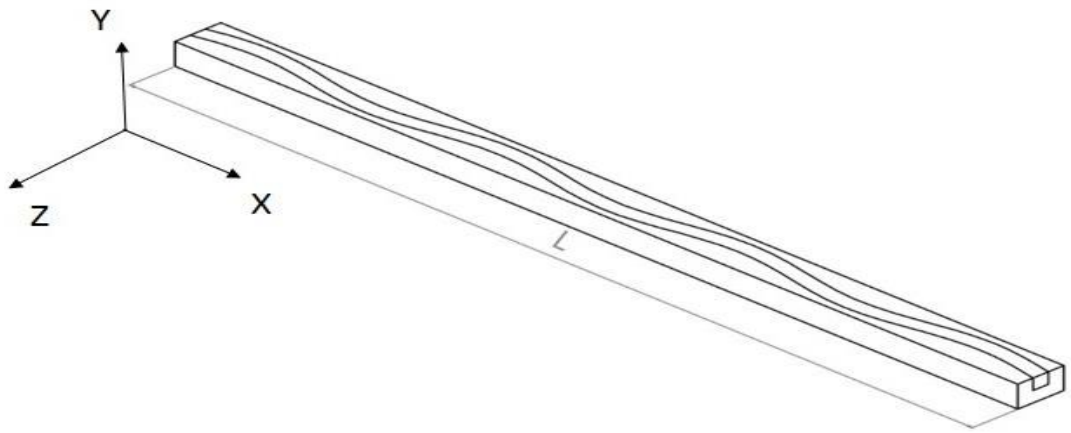

Fig. 3.1: Computational domain

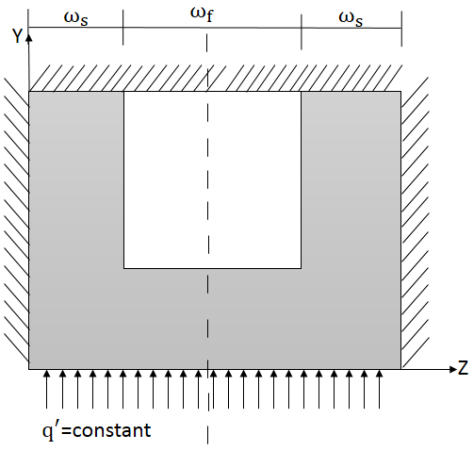

Fig 3.2: Front view of the microchannel

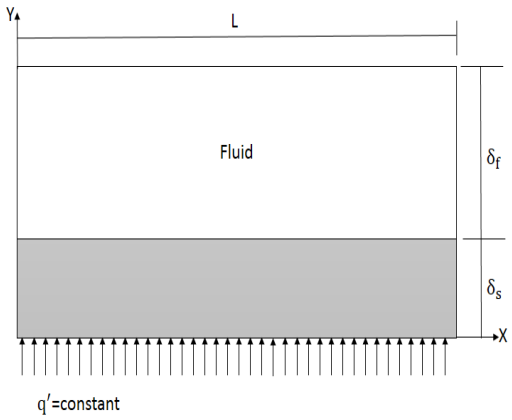

Fig 3.3: Side view of the microchannel

$$U_{in} = U_{av}(1 + A\sin(\omega t))$$

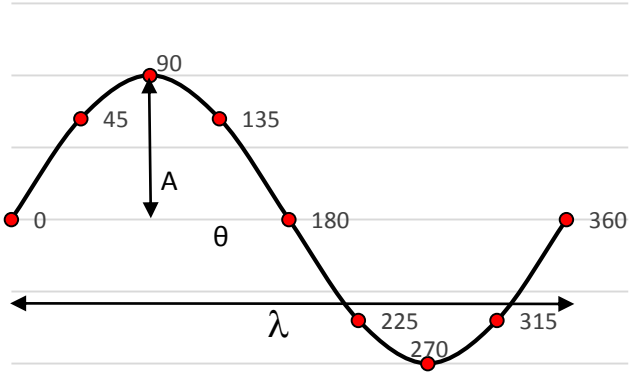

Fig 3.4: Pulsatile inlet velocity

3.1.1 Assumption

Numerical simulations performed out under following assumptions:

- Single phase, laminar incompressible fluid flow.
- Thermo- physical properties of the working fluid are constant.
- Natural convection and radiation mode of heat transfer are neglected.
- Flow is pulsatile i.e. transient.

3.1.2 Governing equations

The flow and heat transfer are governed by the continuity, Navier-Stokes and energy equations. The three-dimensional governing equations of constant thermo-physical properties are written below:

Continuity equation

$$\frac{\partial \rho}{\partial t}+\frac{\partial(\rho u)}{\partial x}+\frac{\partial(\rho v)}{\partial y}+\frac{\partial(\rho w)}{\partial z}=0 \tag{2}$$

Navier-stoke equation

$$\rho\left(\frac{\partial u}{\partial t}+u\frac{\partial u}{\partial x}+v\frac{\partial u}{\partial y}+w\frac{\partial u}{\partial z}\right)=-\frac{\partial P}{\partial x}+\mu\left(\frac{\partial^2 u}{\partial x^2}+\frac{\partial^2 u}{\partial y^2}+\frac{\partial^2 u}{\partial z^2}\right)+F_x \tag{3}$$

$$\rho\left(\frac{\partial v}{\partial t}+u\frac{\partial v}{\partial x}+v\frac{\partial v}{\partial y}+w\frac{\partial v}{\partial z}\right)=-\frac{\partial P}{\partial y}+\mu\left(\frac{\partial^2 v}{\partial x^2}+\frac{\partial^2 v}{\partial y^2}+\frac{\partial^2 v}{\partial z^2}\right)+F_y \tag{4}$$

$$\rho\left(\frac{\partial w}{\partial t}+u\frac{\partial w}{\partial x}+v\frac{\partial w}{\partial y}+w\frac{\partial w}{\partial z}\right)=-\frac{\partial P}{\partial z}+\mu\left(\frac{\partial^2 w}{\partial x^2}+\frac{\partial^2 w}{\partial y^2}+\frac{\partial^2 w}{\partial z^2}\right)+F_z \tag{5}$$

Energy equation

$$\rho c_p\left(\frac{\partial T}{\partial t}+u\frac{\partial T}{\partial x}+v\frac{\partial T}{\partial y}+w\frac{\partial T}{\partial z}\right)=k\left(\frac{\partial^2 T}{\partial x^2}+\frac{\partial^2 T}{\partial y^2}+\frac{\partial^2 T}{\partial z^2}\right)+\Phi \tag{6}$$

where Φ is viscous dissipation factor

$$\Phi=2\mu\left[\left(\frac{\partial u}{\partial x}\right)^2+\left(\frac{\partial v}{\partial y}\right)^2+\left(\frac{\partial w}{\partial z}\right)^2+\frac{1}{2}\left(\frac{\partial v}{\partial x}+\frac{\partial u}{\partial y}\right)^2+\frac{1}{2}\left(\frac{\partial v}{\partial z}+\frac{\partial w}{\partial y}\right)^2+\frac{1}{2}\left(\frac{\partial w}{\partial x}+\frac{\partial u}{\partial z}\right)^2\right] \tag{7}$$

3.1.3 Boundary condition

For liquid domain

$$\nabla.\vec{u}=0 \tag{8}$$

$$\vec{u}.\nabla.\vec{u}=-\frac{1}{\rho}\nabla P+\frac{\mu}{\rho}\nabla^2\vec{u} \tag{9}$$

$$\vec{u}.\nabla.T=(k/\rho.C_p).\nabla^2 T \tag{10}$$

For solid domain

$$\nabla^2 T = 0 \quad (11)$$

$(\partial T / \partial z) = 0$; X-Y plane at z = 0 and z = $2\omega_s + \omega_f$ (12)

$(\partial T / \partial y) = 0$; X-Z plane at y = $(\delta_s + \delta_f)$ (13)

$(\partial T / \partial x) = 0$; Y-Z plane at x = 0 and x = L (14)

q' = constant; X-Z plane at y = 0 (15)

$u = u_{av}(1 + A.\sin(\omega t))$; Y-Z plane at x = 0 (16)

$u = 0$; at solid liquid interface (17)

3.2 CFD modelling

The commercial software package ANSYS Fluent® solved all governing equations discussed above which is based on the finite volume method discretization.

3.2.1 Geometry Creation

The computational domain of the parallel wavy micro channel of dimensions (L = 30 mm and D_h = 0.4 mm) in 3D is created with the help of SOLID WORKS software package. In SOLID WORKS, with the help of equation of spine line button, the curve is created on the top plane. Then, copy that line to 0.4 mm distance. Then, edges are joined by lines to create a face which is then extruded by 0.4 mm distance. This resulted in the creation of one part (fluid channel). The other part is created by directly creating a rectangle of (L = 30 mm and width 1.2 mm) and on the top surface same wavy face is created. Then extrude cut that surface from rectangle, which results in the generation of the solid substrate. Finally assemble the two parts by "coincide" option by selecting one common point of two parts. The computational domain is then imported in DESIGN MODELER (DM) screen for further simulation. Then change all the units in 'mm'. Then go to meshing in which naming should be done as per shown diagram given below.

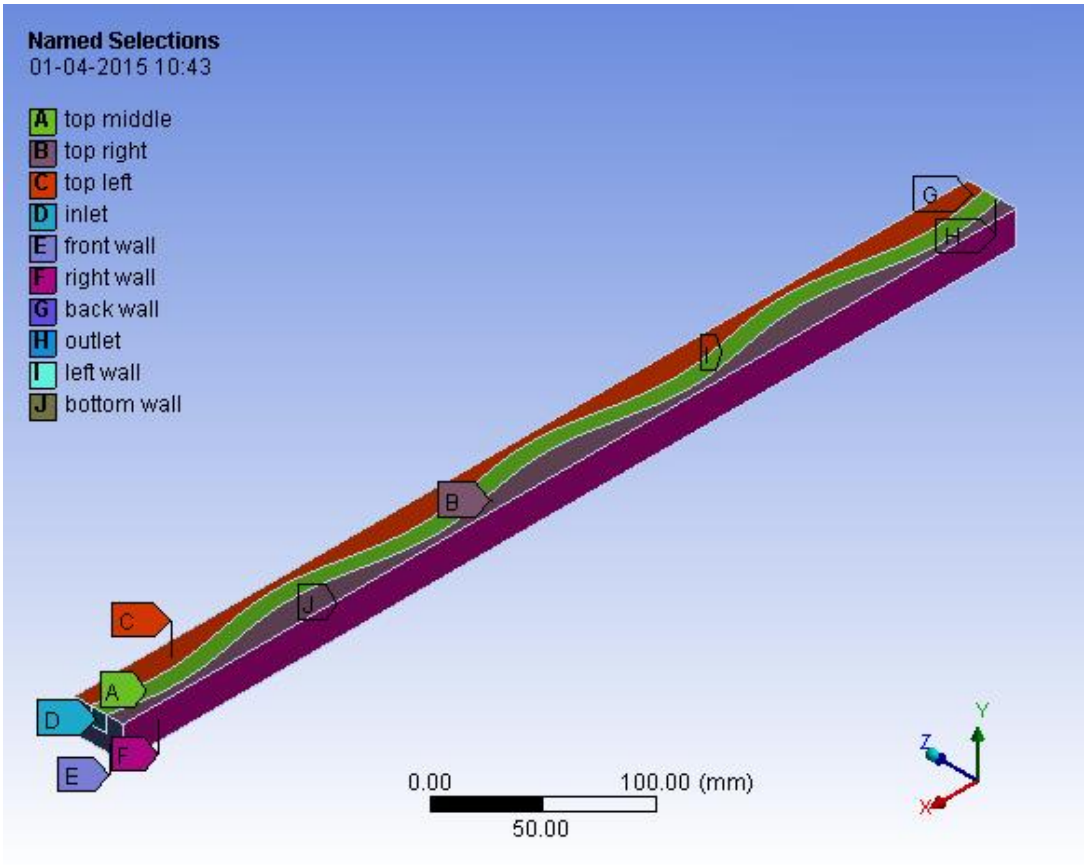

Fig. 3.5: Named boundary of computational domain

3.2.2 Grid Generation

The quality of the mesh is very important to get the good result as it affects the level of accuracy. Hence after the creation of geometry model in SOLIDWORKS, it is imported into GEOMETRY MODELLER. Then close the GEOMETRY MODELLER and open the MESH in WORK BENCH, which reads the geometry file automatically. After that in MESH window click on GENERATED MESH button, default mesh is generated, which is further controlled by MESH CONTROL by EDGE SIZING and in addition MAPPED FACING option should be incorporated by clicking on the MAPPED FACE button. The behaviour of mesh changes from SOFT to HARD and the bias type is "No Bias". Export the mesh file name as Name**.**msh in Fluent Input File. The enlarged view of the meshed domain is shown below.

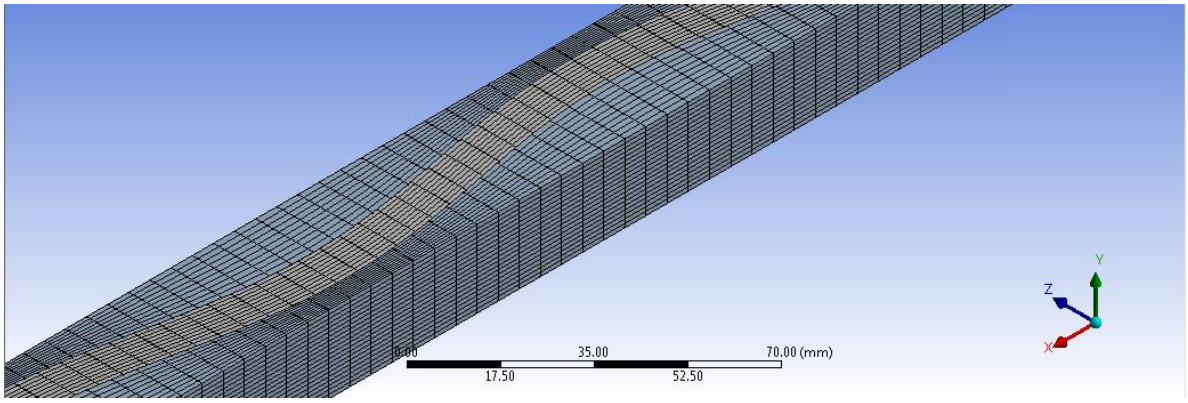

Fig. 3.6: Meshing of computational domain

3.2.2.1 Grid independence test

Grid independence test is performed to check whether the grid size gives an accurate result or not. After the grid independence test, the grid size is used for all simulations. In this case of pulsatile flow inlet, local Nusselt number [Nu(z,t)] is calculated for one phase angle 90° where Re = 100, frequency = 2 Hz and δ_{sf} = 1 for three different grid sizes 14 × 105, 16 × 120 and 20 × 150.

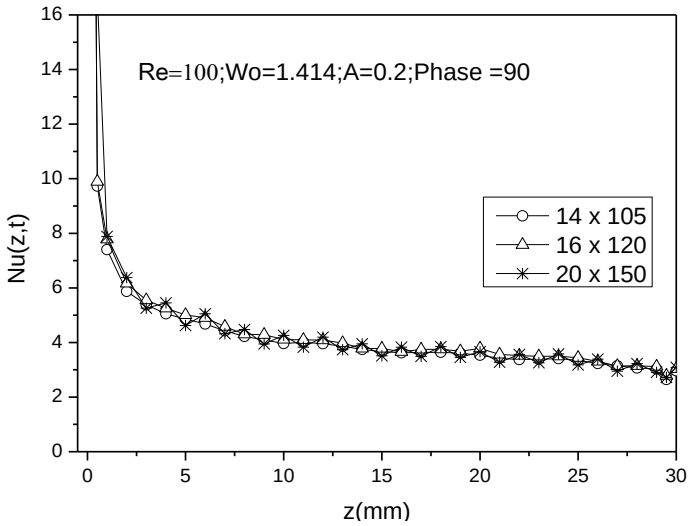

Fig. 3.7: Grid independence test

From the above graph increasing the grid size from 14 × 105 to 16 × 120, instantaneous local Nusselt number [Nu (z,t)] decreased by 0.4%, but by further increasing the grid size from 16 × 120 to 20 × 150, the percentage difference local Nusselt number [Nu(z,t)] was reduced to 3.12%. So by considering the percentage change of local Nusselt number [Nu(z,t)] it was confirmed that grid size '16 × 120' should be used for simulation.

3.2.3 Setup and flow specification

Open the fluent set up in 3D double precision mode for higher accuracy and then read the exported mesh file, click on the transient button as the problem is unsteady (pulsatile) flow. Solver type is pressure based, and absolute velocity formulation are default set. In model switch on the energy as the problem involves heat transfer while the others remain the same. In material section change fluid from air to water from fluent database whose properties are given below:

Table 3.1: Thermo- physical properties of water

Property	Symbol	Value	Unit
Specific heat at constant pressure	C_p	4180	J/kg-K
Thermal conductivity	k_f	0.6	W/m-K
Dynamic viscosity	μ	0.001003	Kg/m-s
Density	ρ	998.2	Kg/m^3

After selecting the fluid, different solid materials are chosen for wall of solid substrate having properties are listed below:

Table 3.2: Thermo- physical properties of solid substrate

Solid Name	**ρ (Kg/m^3)**	**C_p (J/kg-K)**	**k_s (W/m-K)**	**k_{sf} (k_s/k_f)**
Sulphur	2070	708	0.206	0.344
Silicon dioxide	2220	745	1.38	2.3
Bismuth	9780	112	7.86	13.1
SS316	8238	468	13.4	22.33
Constantan	8920	384	23	38.34
Bronze	8780	355	54	90
Zink	7140	389	116	193.33
Aluminium	2719	871	202.4	337.33
Silver	10,500	235	429	715

After choosing the material, go to cell zone condition in which fluid type changes from air to water. As the problem is unsteady interpret the user-defined function (UDF) which is saved as .C extension in the same file. After that go to boundary condition and change the inlet to "udf unsteady_velocity", also cross check the conjugate wall which is shown in thermal condition 'coupled'.

3.2.4 Solution

In the solution method pressure-velocity coupling scheme is 'SIMPLE', the second order upwind scheme is used for energy and momentum equations in order to achieve higher accuracy. The gradient method is 'Green-Gauss Cell Based'. In solution control the under relaxation factors keep as default shown below:

Table 3.3: Value of under relaxation factors

Pressure	Density	Body force	Momentum	Energy
0.3	1	1	0.7	1

The convergence criteria of momentum and energy equations are set 10^{-6} and 10^{-9} respectively. In reference value set compute from the inlet. Solution initialization scheme is standard and compute from the inlet. For extraction of each time step data of any cycle use, auto save option is used to save each data file. Set autosave at every time step i.e. 1. In run calculation time step size is calculated for different frequencies of pulsation, maximum iteration per time step is set to 1000 for convergence and set the number of time steps to obtain a steady periodic solution.

3.3 Data reduction

The parameters are (a) local heat flux for a different phase angle for a cycle (b) local wall and bulk fluid temperature for a different phase angle for a particular cycle. These parameters help us to examine the effect of axial back conduction on local Nusselt number where conductivity ratio (k_{sf}) play an important role.

Axial coordinate (x) in dimensionless form written as

$$z^* = \frac{x}{L} \tag{18}$$

The dimensionless heat flux at solid-fluid interface is written as

$$\phi = \frac{q_z}{\overline{q'}} \tag{19}$$

where q_z is the value of local heat flux at each axial location of z^*, $\overline{q'}$ is the ratio of applied heat flux at the bottom of solid substrate and net area of conjugate walls, given by

$$(\overline{q'}) = (q').(2\omega_s + \omega_f) / (2\delta_f + \omega_f) \tag{20}$$

where, q' is the wall heat flux applied at the bottom of the solid substrate.

Dimensionless wall and bulk fluid temperature are given as

$$\Theta_w = \frac{T_{wz} - T_{fi}}{T_{fo} - T_{fi}} \tag{21}$$

$$\Theta_f = \frac{T_{fz} - T_{fi}}{T_{fo} - T_{fi}} \tag{22}$$

where T_{wz} and T_{fz} are wall and average bulk fluid temperature at any location of z^* of the channel. T_{fi} and T_{f0} are the average bulk fluid temperature at the inlet and outlet respectively.

Instantaneous local Nusselt number is

$$Nu(z,t) = \frac{h(z,t).D_h}{k_f} \tag{23}$$

where $h(z,t)$ is the local heat transfer coefficient which is given by

$$h(z,t) = \frac{q_z}{T_w - T_f} \tag{24}$$

The space average local Nusselt number is given by

$$\mathrm{Nu}(z,t) = \frac{1}{L}\int_0^L \mathrm{Nu}(z,t)\,dz \tag{25}$$

The time average local Nusselt number is given by

$$\mathrm{Nu}(z,t) = \frac{1}{\theta}\int_0^\theta \mathrm{Nu}(z,t)\,dt \tag{26}$$

The overall Nusselt number is given by

$$\mathrm{Nu}_{avg} = \frac{1}{L\theta}\int_0^\theta\int_0^L \mathrm{Nu}(z,t)\,dt\,dz \tag{27}$$

Relative Nusselt number is given by

$$\mathrm{Nu}_r = \frac{\mathrm{Nu}_t}{\mathrm{Nu}_s} \tag{28}$$

where Nu_t and Nu_s are transient and steady state Nusselt number respectively.

Chapter-4

Result and discussion

Simulation done by using water as working fluid that enter into the channel at 300 K, flow rate Re = 100 and Pr = 7 with pulsatile velocity i.e. vary sinusoidally with time. To get the steady solution, all data were extracted at a particular cycle (5_{th}) for different phase angle ranges from 0 to 360.

The analysis done for see result by using pulsatile velocity UDF is similar to theoretical value or not. Simulation done for particular pulsation frequency f = 2 Hz (Wo = 1.414) with different amplitude 0.2 and 0.4. By the simulation, it has found that obtained results similar to theoretical results.

Fig. 4.1 shows radial velocity for a different phase angle by varying amplitude from 0.2 to 0.4 in the fully developed region. From the graph, it has found that velocity is maximum at phase angle 90 and minimum at phase angle 270 which is theoretically correct. In upper part of velocity cycle phase angle from 45 to 135 shows by increasing amplitude velocity increases [fig 4.1(a-c)] and for lower part of velocity cycle phase angle from 225 to 315 shows by increasing amplitude velocity decreases.

In Fig. 4.2 it clear that for phase angle 0,180 and 360 velocity overlap, which coincide with theoretical pulsatile velocity inlet value. Also velocity at phase angle 45 & 135 and 225 & 315 overlap separately. Here no inertia effect is found as per [40] because of the wavy wall of the microchannel.

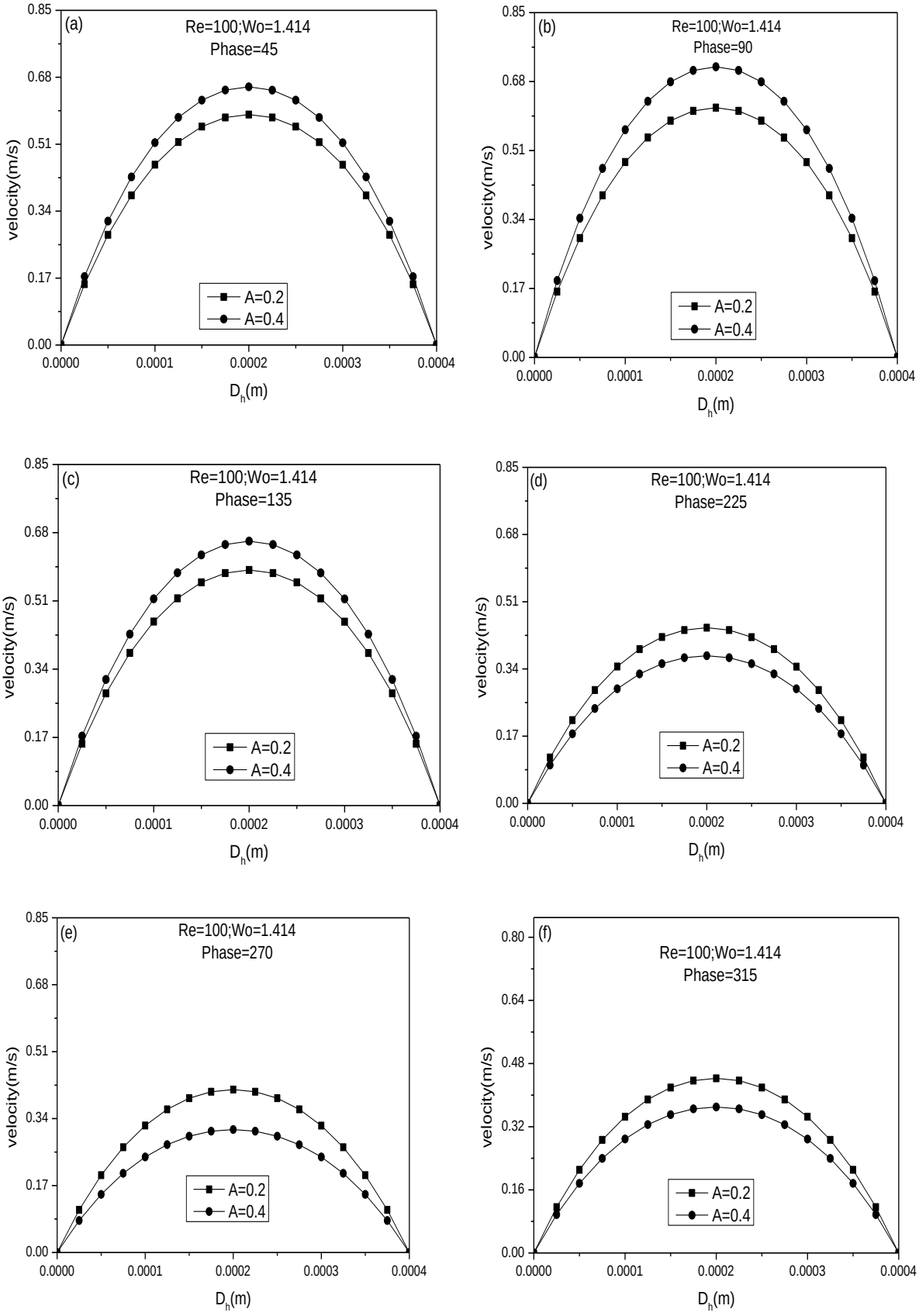

Fig. 4.1: Velocity variation at different phase angle for two different amplitude

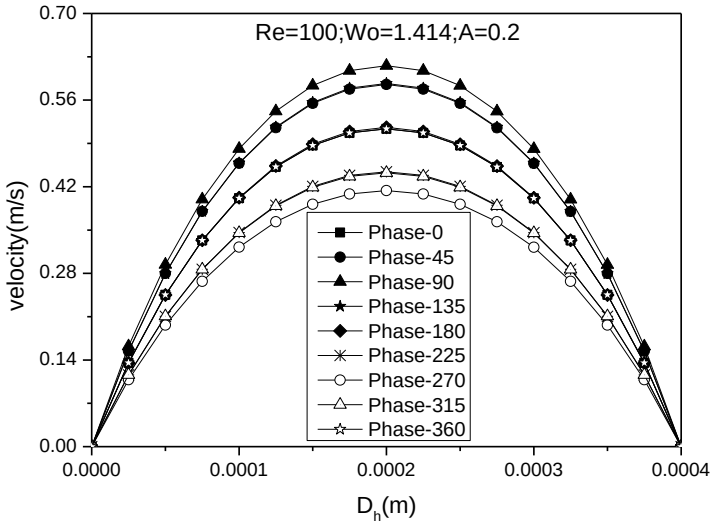

Fig. 4.2: Variation of velocity magnitude for different phase angle (0-360)

From the different literature, it was found that k_{sf} plays a key to enhancing axial wall conduction or conjugate heat transfer in a microchannel, where they carried out the simulation for different k_{sf} values. Similarly here simulation carried out for wide ranges of k_{sf} from 0.344 to 715.

Variation of dimensionless heat flux (ϕ) along the axial direction for different k_{sf} values from 0.344 to 715 show in figure 4.3. As the microchannel having some finite thickness, that is more than a conventional channel, the heat flux applied at the bottom of solid substrate not equal to the heat flux experienced at the solid-fluid interface. The variation also shows for phase angle 0, 90 and 270 at a Wo = 2 (pulsation frequency = 2 Hz).

Heat flux experienced at the solid-fluid interface at low k_{sf} show a drastic change i.e. heat flux is more than the applied heat flux value. The effect of axial wall conduction is increased proportional with k_{sf} value which is overlap with zero wall thickness wall at k_{sf} = 13.1.The value of heat flux at solid-fluid interface decreased at the outlet of the channel with increasing k_{sf} because by increasing k_{sf} value thermal resistance of the substrate channel decreases leads to decrease in heat flux as Fig. 4.3 (c-f).

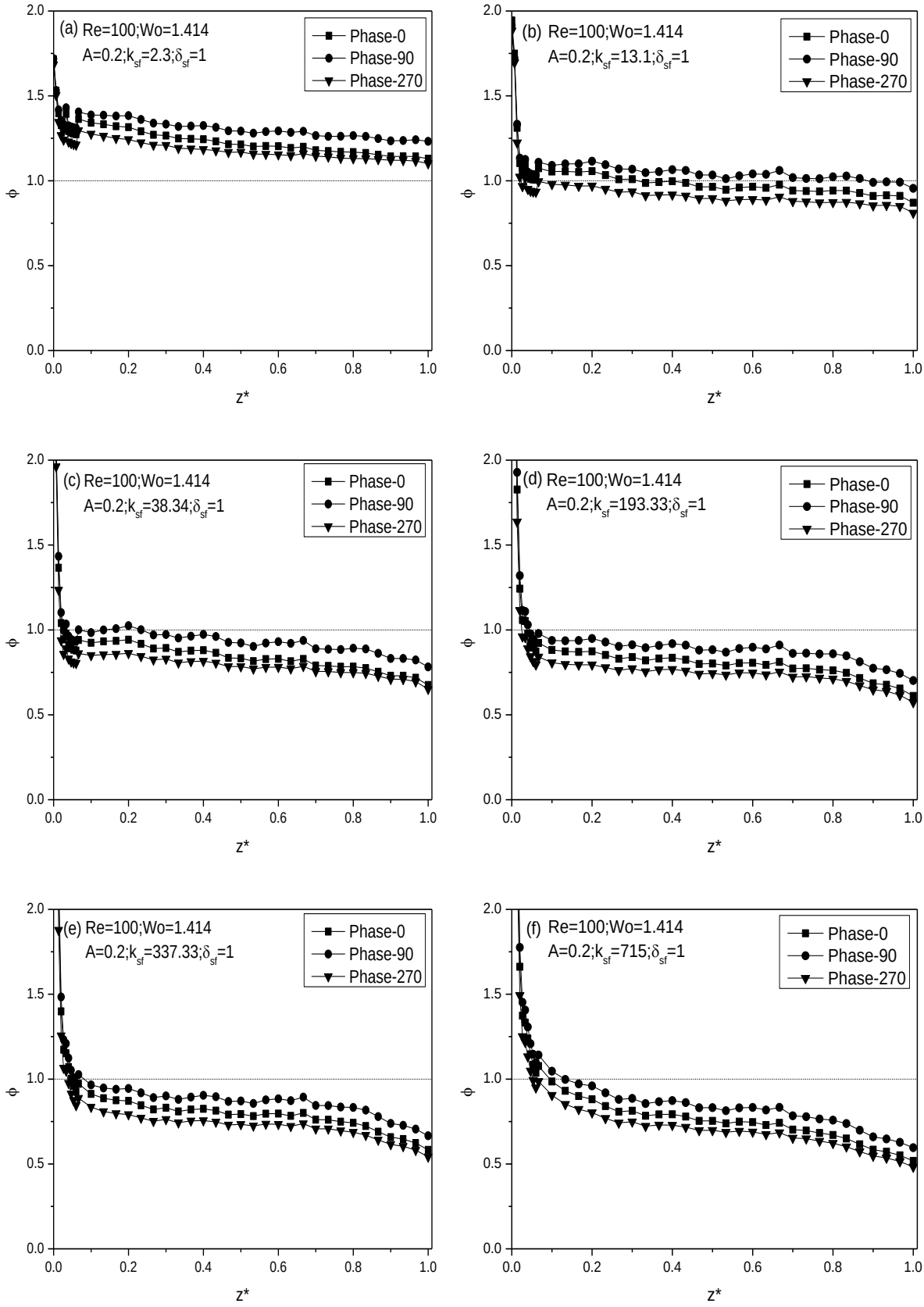

Fig. 4.3: Dimensionless heat flux variation in axial direction for different k_{sf} values.

By increasing phase angle from 0 to 90 show that dimensionless heat flux at the solid-fluid interface increases slightly and decreases slightly by further increase from 90 to 270. The above results found because as per pulsatile velocity inlet velocity magnitude is maximum at phase angle 90 and minimum at 270.

The variation of dimensionless fluid temperature and wall temperature at the solid-fluid interface for wide range of k_{sf} from 0.344 to 715 for f = 2 Hz corresponding Wo = 1.414 shown in Fig. 4.4. For ideal condition flow through a circular tube subjected to constant wall heat flux boundary condition on outer wall results variation of bulk fluid temperature and wall temperature variation along the length of tube is linear in fully developed region i.e. difference between wall and bulk fluid temperature is constant in fully developed region. At low k_{sf} Fig. 4.4(a) it is observed that the difference between fluid and wall temperature gradually increases towards the end of the channel due to the wavy wall. In case of high k_{sf} value, the conventional theory does not valid because of the larger temperature of an outlet than the inlet of working fluid lead to conduction in the opposite direction to fluid flow. The wall temperature increases by the changing phase angle from 0 to 90 same as [24], but the variation is not found in the case of bulk fluid temperature that does not vary with phase angle. Again by the changing phase angle from 90 to 270 show that wall temperature decreases from initial value i.e. at phase angle 0. It is obtained that by increasing k_{sf} the wall temperature value decreases.

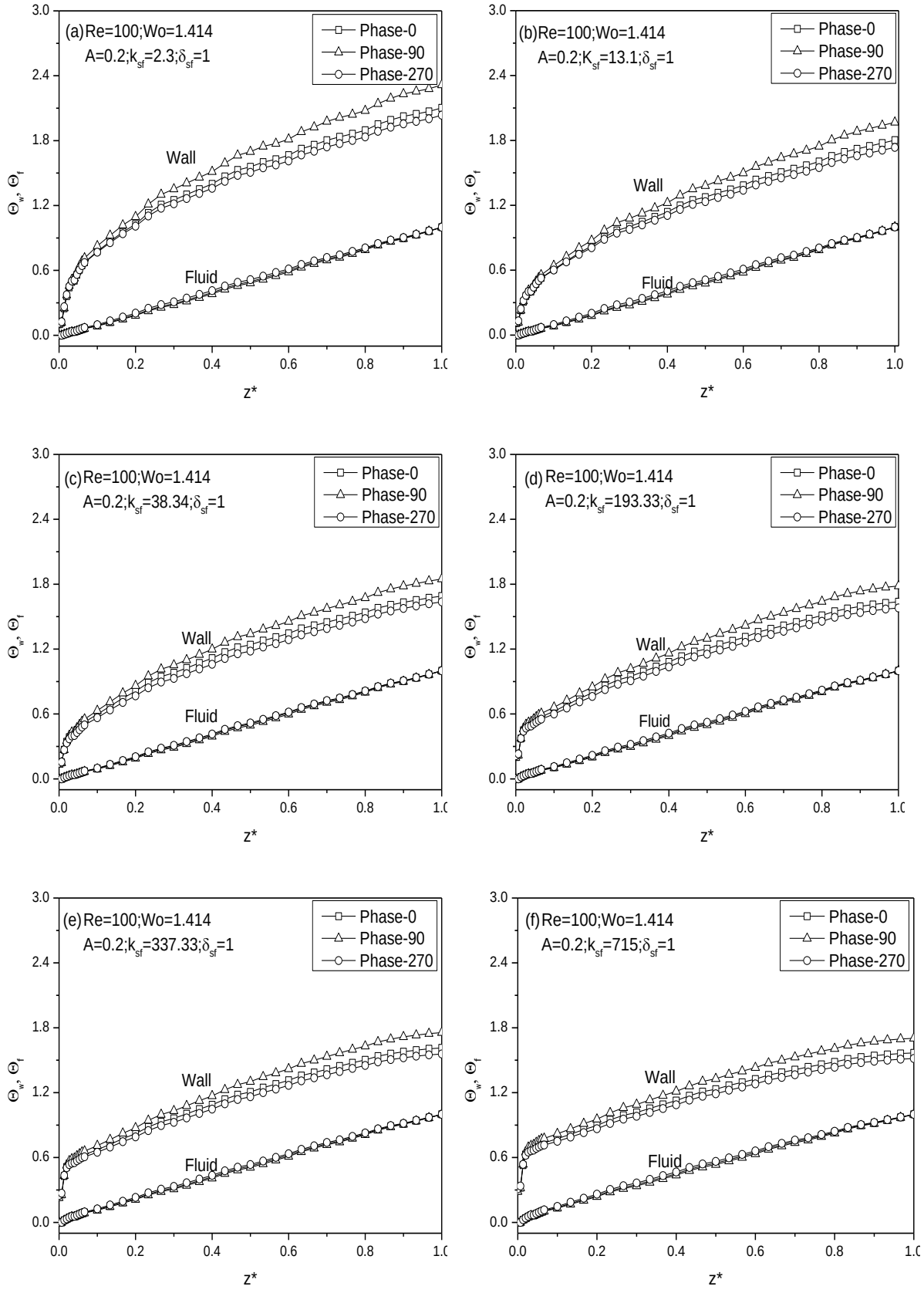

Fig. 4.4: Dimensionless bulk fluid and wall temperature variation in axial direction for different k_{sf} values.

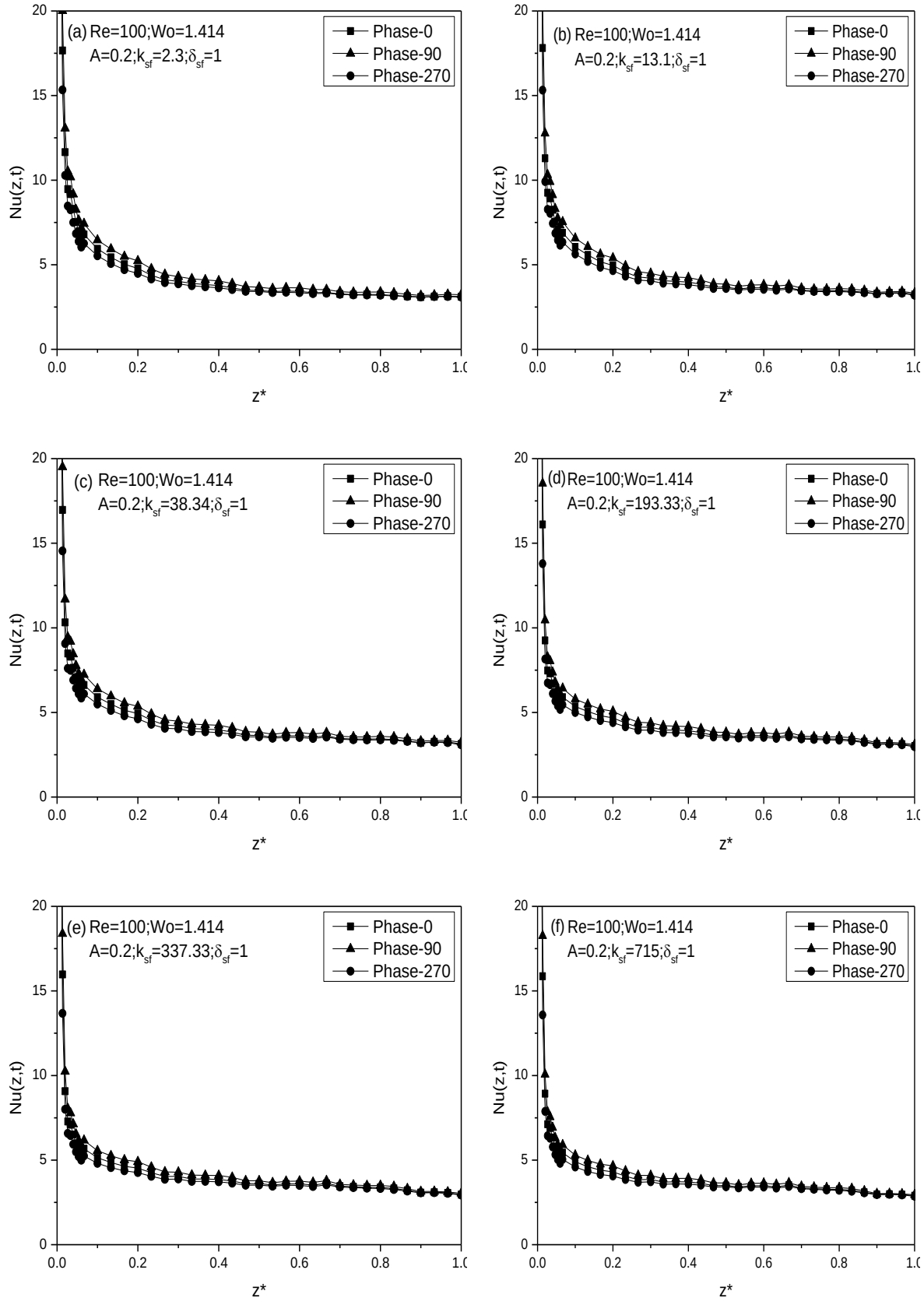

Fig. 4.5: Local Nusselt number variation in axial direction for different k_{sf} values.

Axial variation of local Nusselt number for different k_{sf} value at phase angle 0, 90 and 270 shown in Fig. 4.5. The simulation did for Re = 100 and f = 2 Hz followed by Wo = 1.414.There is no appreciable change in Nusselt number with k_{sf}. When phase angle change from 0 to 90 the local Nusselt number value increases slightly and further decreases slightly by the changing phase angle from 90 to 270. The above result is observed because at phase angle 90 magnitude of velocity is maximum that causes proper mixing of fluid leads to increase heat transfer and at phase angle 270 magnitude of velocity is minimum leads to lower heat transfer.

Variation of average local Nusselt number [Nu(t)] at a different phase angle for every k_{sf} value shown separately in Fig. 4.6. It is observed that for all k_{sf} the average Nusselt number vary periodically same as the sinusoidally varying pulsatile velocity inlet i.e. Nu(t) increases by increase phase angle from 0 to 180 (upper part of cycle) and further decrease by increasing phase angle from 180 to 360(lower part of cycle). It is also obtained that by increasing k_{sf} from 2.3 to 13.1 Nu(t) value increases which is further decreases by increase in k_{sf} from 13.1 to 715 due to conjugate heat transfer or axial wall conduction effect.

Fig. 4.7 shows the simulated result of time average relative Nusselt number [$Nu_r(z)$] variation for all k_{sf} values ranging from 2.3 to 715 at pulsating frequency (f = 4 Hz, Wo = 2). For low k_{sf} = 2.3 $Nu_r(z)$ fluctuating thought out the channel, but at k_{sf} = 13.1 $Nu_r(z)$ vary smoothly along the channel which is less than one which indicate $Nu_r(z)$ is less compared to steady case. In developing zone $Nu_r(z)$ less than one which is gradually increasing in the fully developed zone. By increasing k_{sf} from 13.1 to 22.33 the $Nu_r(z)$ value, suddenly decreases which is further increased by increasing k_{sf} from 22.33 to 715. For all k_{sf} except 13.1 $Nu_r(z)$ increases at the outlet zone.

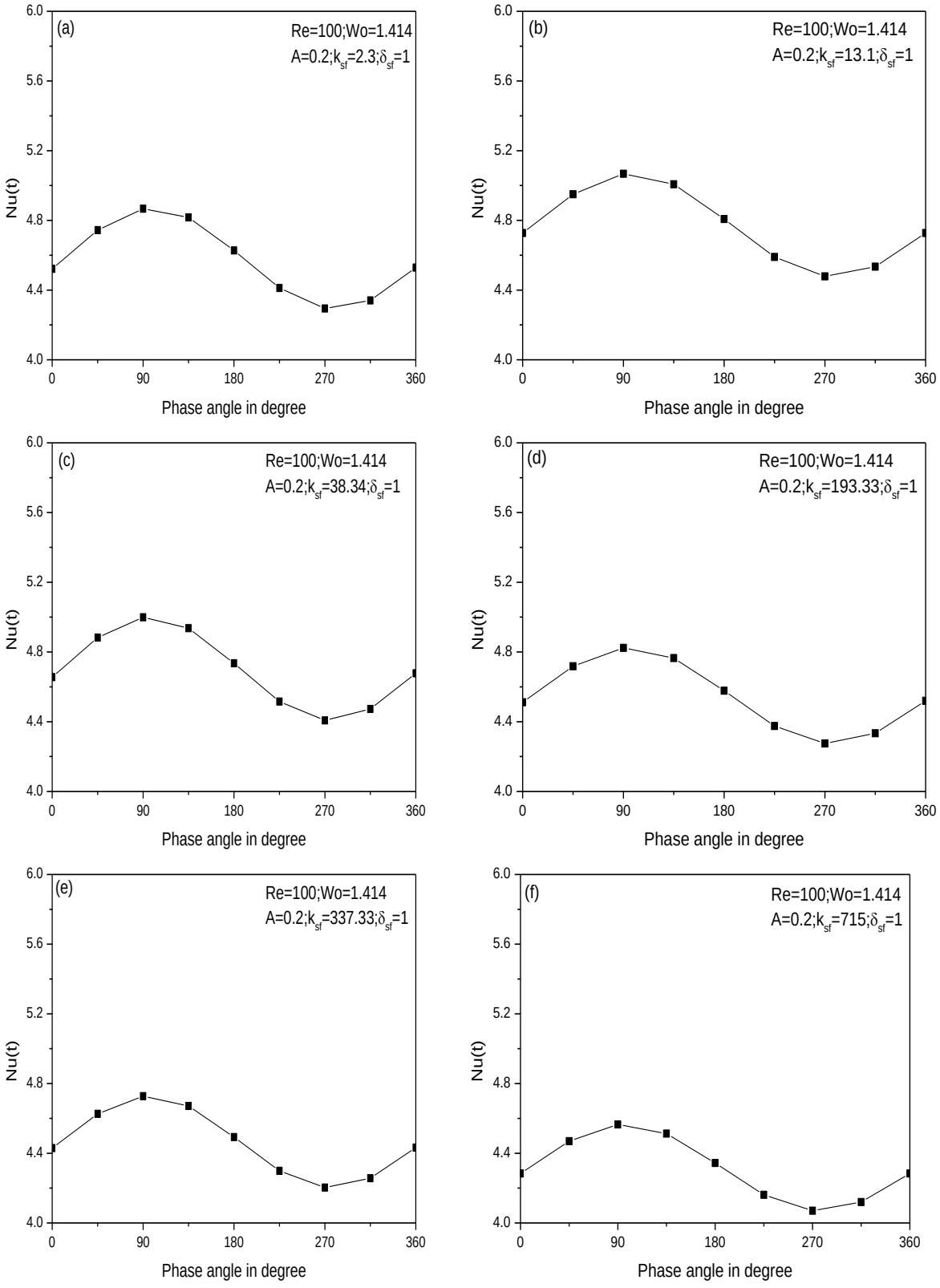

Fig. 4.6: Variation of space average local Nusselt number [Nu(t)] in axial direction for different k_{sf} values.

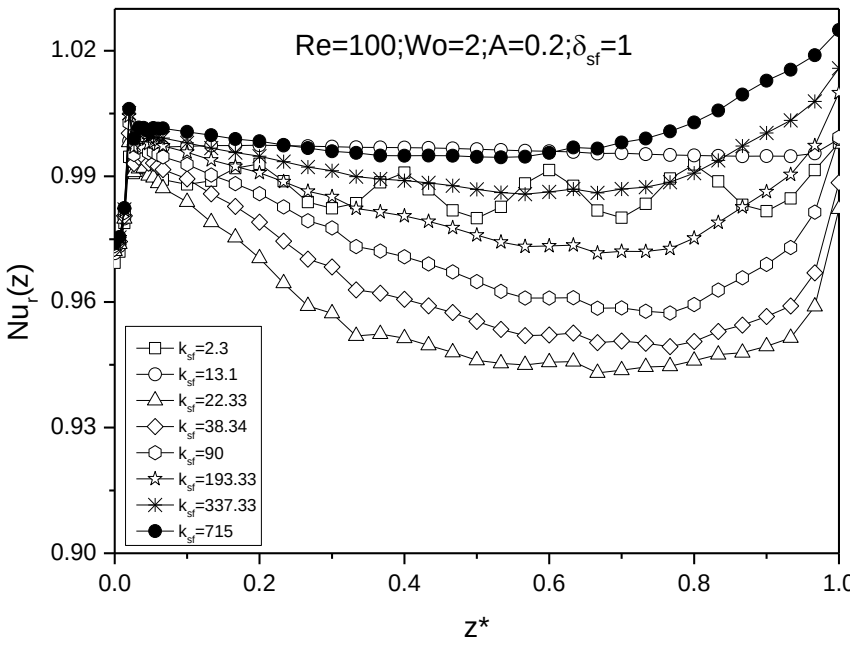

Fig. 4.7: Time average relative Nusselt number variation for all k_{sf} values.

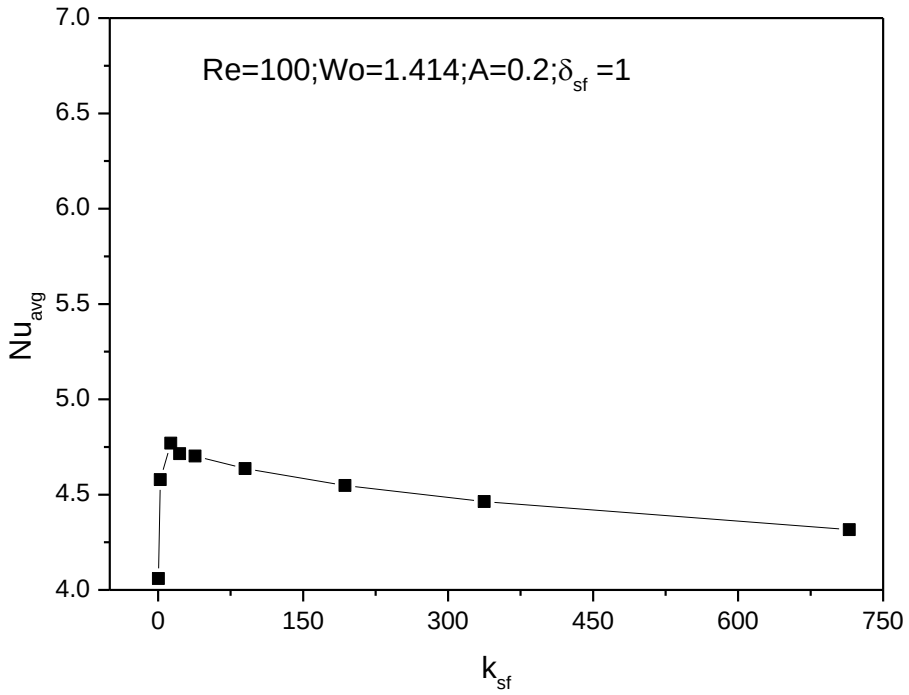

Fig. 4.8: Variation of overall Nusselt number with k_{sf}

The Fig. 4.8 shows the optimum k_{sf} value at which Nu is maximum. Fig. 4.8 shows variation overall Nusselt number for all k_{sf} value from 0.344 to 715 at particular pulsating frequency, f = 2 Hz (Wo = 1.414). The value of Nu_{avg} increases rapidly up to an optimum value from low k_{sf} value 0.344 after optimum value the Nu value decrease due to axial wall conduction in the solid substrate of the microchannel. It is obtained that there exist an optimum k_{sf} where Nu value is maximum. The overall Nu variation in line with literature by Moharana M. K. et al. [21], Moharana, M. K., & Khandekar [22], Yadav et al. [23] where the steady flow inlet but in Mishra, P., & Moharana, M. K [24] and [40] inlet velocity is pulsatile.

Fig. 4.9 shows variation of relative local Nusselt number along channel length at particular k_{sf} = 13.1 for different pulsation frequency i.e. (f = 2, 4, 6 and 10 Hz) correspond Wo = 1.414, 2, 2.45 and 3.163 respectively. The pulsation effect is more in developing the region, so the oscillation is more in that region which decrease towards developed region. From Fig.4. 9 (a-d) it was found that $Nu_r(z,t)$ value of positive half-cycle phase angles (45, 90, 135) is higher than $Nu_r(z,t)$ value at negative half-cycle phase angles(225, 270, 315).It is also observed that for low pulsation frequency (f = 2 Hz, Wo = 1.414) $Nu_r(z,t)$ vary widely towards the end of channel [Fig.4.9(a)], However, by increasing pulsation frequency they converge[Fig. 4.9(b-d)]. At higher pulsation frequency i.e. Wo = 2.45 and 3.163 $Nu_r(z,t)$ value increases at outlet [Fig. 4.9(c-d)]. In Fig. 4.9 all the graphs are fluctuating or zigzag due to the wavy wall of the substrate channel.

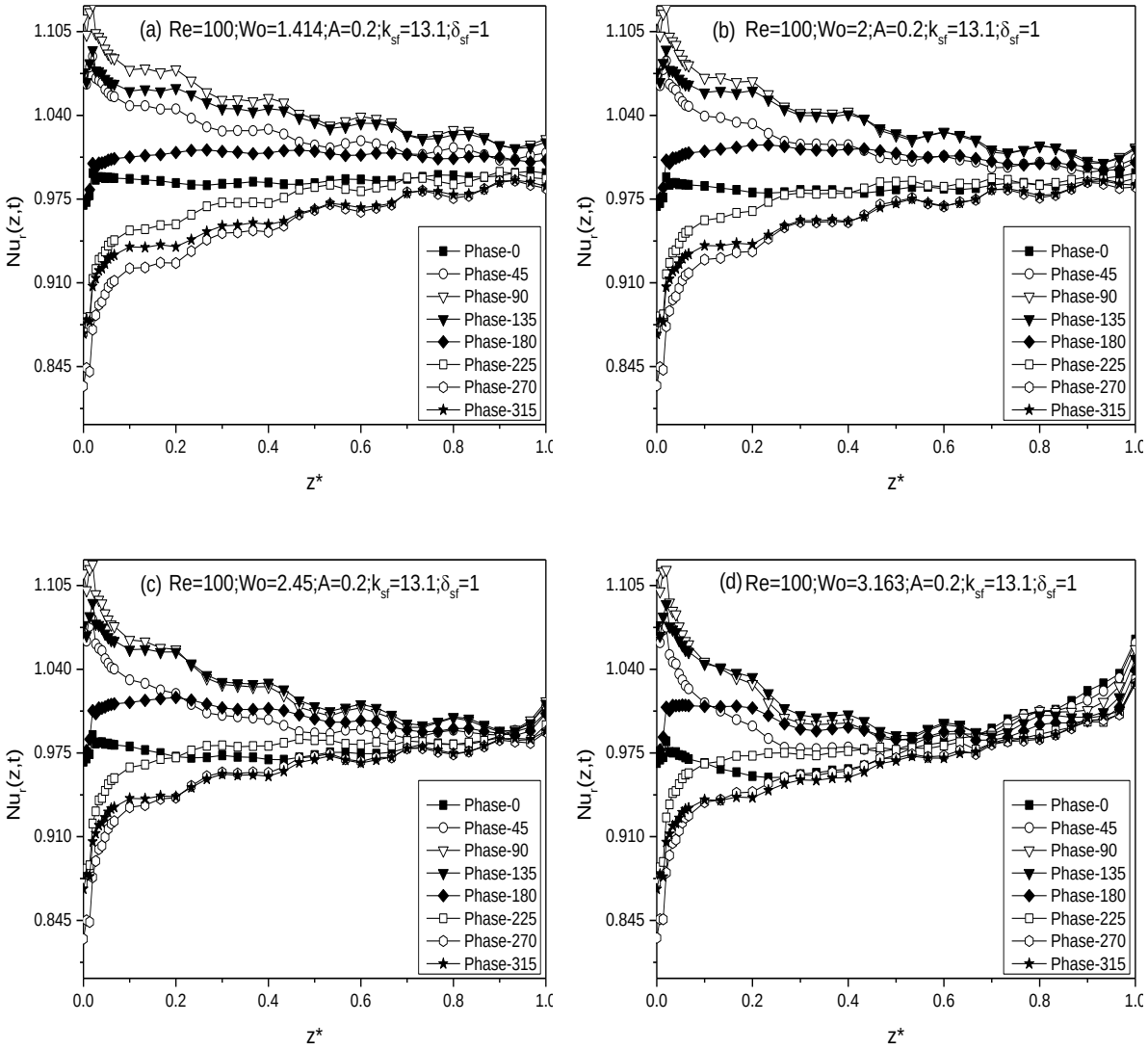

Fig. 4.9: Variation of relative local Nusselt number at particular k_{sf} = 13.1 for different pulsation frequency

Chapter-5

Conclusion and future scope

A numerical simulation carried out to show the effect of pulsatile velocity inlet on axial wall conduction for laminar flow through in a microchannel subjected to constant wall heat flux boundary condition at the bottom of the solid substrate. Simulation done for a wide range of conductivity ratio k_{sf} from 0.344 to 715, thickness ratio (δ_{sf} = 1, 2) and flow rate (Re = 100, 200) while the amplitude of pulsatile velocity fixed (A = 0.2). To observed the effect of pulsation, the pulsation frequency vary i.e. f = 2, 4, 6 and 10Hz corresponding Womersley number = 1.414, 2, 2.45 and 3.163 respectively. From the numerical simulation conclusions are observed as follows:

- Because of sinusoidally pulsatile velocity inlet it is observed that the magnitude of velocity is maximum at phase angle 90 and minimum at phase angle 270.The velocity profile overlaps for phase angle 45 & 135, 225 & 315 and 0, 180 & 360 separately as shown in Fig. 4.2 similar to pulsatile inlet condition.
- By increasing k_{sf} value the dimensionless wall temperature decreases and the profile not similar to conventional one due to conjugate heat transfer.
- The dimensionless heat flux value decrease towards outlet by an increase in k_{sf} due effect of conjugate heat transfer.
- The effect of change of pulsation frequency is very less in case of Nu.
- The value of relative local Nu is more inside the developing region which is coverage toward the outlet. By increasing frequency, the Relative Nu converges more than low

frequency. At high frequency = 10 Hz, the relative Nu values increase at outlet due increase in axial wall conduction.

- The space average local Nusselt number [Nu (t)] decrease with an increase in and varies sinusoidally same as pulsatile velocity inlet k_{sf}.
- For a particular value of Wo at low k_{sf} the overall Nusselt number (Nu_{avg}) is small.
- The value of overall Nu is maximum at a moderate value of k_{sf} which is lower than that of Mishra & Moharana [24].
- By increasing the k_{sf} value beyond optimum value, the overall Nu decreases due to the effect of conjugate heat transfer leads to increase axial wall conduction.
- Overall Nu is function of Re and thickness ratio δ_{sf} at particular Wo.

As per modern days, there are many practical applications of pulsatile flow in the engineering field. Using multiphase is the future scope of the project. Also the analysis will be done for very high and low Re, higher value of frequency, wide range of amplitude of velocity inlet and shape of the channel also change from parallel wavy to raccoon channel i.e. crest and tough facing each other by phase angle 0°. Boundary condition of the problem may be change to constant wall temperature condition and partial heated boundary condition or may be heating in more than one surface will be done.

References:

1. Khandekar, S. and Moharana, M. K, (2014), Some Applications of Micromachining in Thermal-Fluid Engineering, Chapter in: Introduction to Micromachining, 2nd Edition, Editor: Dr. V. K. Jain, Narosa Publishing House.
2. Uchida, S. (1956). The pulsating viscous flow superposed on the steady laminar motion of incompressible fluid in a circular pipe. Zeitschrift für angewandte Mathematik und Physik ZAMP, 7(5), 403-422.
3. Al-Haddad, A. A., & Al-Binally, N. (1989). Prediction of heat transfer coefficient in pulsating flow. International Journal of Heat and Fluid Flow, 10(2), 131-133.
4. Siegel, R., & Perlmutter, M. (1962). Heat transfer for pulsating laminar duct flow. Journal of Heat Transfer, 84(2), 111-122.
5. Faghri, M., Javdani, K., & Faghri, A. (1979). Heat transfer with laminar pulsating flow in a pipe. Letters in Heat and Mass Transfer, 6(4), 259-270.
6. Karamercan, O. E., & Gainer, J. L. (1979). The effect of pulsations on heat transfer. Industrial & Engineering Chemistry Fundamentals, 18(1), 11-15.
7. Cho, H. W., & Hyun, J. M. (1990). Numerical solutions of pulsating flow and heat transfer characteristics in a pipe. International Journal of Heat and Fluid Flow, 11(4), 321-330.
8. Kim, S. Y., Kang, B. H., & Hyun, J. M. (1993). Heat transfer in the thermally developing region of a pulsating channel flow. International Journal of Heat and Mass Transfer, 36(17), 4257-4266.
9. Moschandreou, T., & Zamir, M. (1997). Heat transfer in a tube with pulsating flow and constant heat flux. International Journal of Heat and Mass Transfer, 40(10), 2461-2466.

10. Hemida, H. N., Sabry, M. N., Abdel-Rahim, A., & Mansour, H. (2002). Theoretical analysis of heat transfer in laminar pulsating flow. International Journal of Heat and Mass Transfer, 45(8), 1767-1780.
11. Yu, J. C., Li, Z. X., & Zhao, T. S. (2004). An analytical study of pulsating laminar heat convection in a circular tube with constant heat flux. International Journal of Heat and Mass Transfer, 47(24), 5297-5301.
12. Chattopadhyay, H., Durst, F., & Ray, S. (2006). Analysis of heat transfer in simultaneously developing pulsating laminar flow in a pipe with constant wall temperature. International Communications in Heat and Mass Transfer, 33(4), 475-481.
13. Mehta, B., & Khandekar, S. (2010, January). Effect of periodic pulsations on heat transfer in simultaneously developing laminar flows: A numerical study. In 2010 14th International Heat Transfer Conference (pp. 569-576). American Society of Mechanical Engineers.
14. Persoons, T., Saenen, T., Donose, R., & Baelmans, M. (2009, October). Heat transfer enhancement due to pulsating flow in a microchannel heat sink. In Thermal Investigations of ICs and Systems, 2009. THERMINIC 2009. 15th International Workshop on (pp. 163-167). IEEE.
15. Kumar, N., & Agrawal, A. (2009). Study of blood flow in microchannels. Proceedings ICCMS09, IIT Bombay, 1-2.
16. Maranzana, G., Perry, I., & Maillet, D. (2004). Mini-and micro-channels: influence of axial conduction in the walls. International Journal of Heat and Mass Transfer, 47(17), 3993-4004.
17. Zhang, S. X., He, Y. L., Lauriat, G., & Tao, W. Q. (2010). Numerical studies of simultaneously developing laminar flow and heat transfer in microtubes with thick wall and constant outside wall temperature. International Journal of Heat and Mass Transfer, 53(19), 3977-3989.

18. Cole, K. D., & Çetin, B. (2011). The effect of axial conduction on heat transfer in a liquid microchannel flow. International Journal of Heat and Mass Transfer, 54(11), 2542-2549.
19. Moharana, M. K., Agarwal, G., & Khandekar, S. (2011). Axial conduction in single-phase simultaneously developing flow in a rectangular mini-channel array. International Journal of Thermal Sciences, 50(6), 1001-1012.
20. Moharana M. K. and Khandekar S., (2013), Numerical study of axial back conduction in microtubes, In Proceedings of the Thirty-Ninth National Conference on Fluid Mechanics and Fluid Power, December 13-15, SVNIT Surat, Gujarat, India: Paper number FMFP2012 – 135.
21. Moharana, M. K., Singh, P. K., & Khandekar, S. (2012). Optimum Nusselt number for simultaneously developing internal flow under conjugate conditions in a square microchannel. Journal of Heat Transfer, 134(7), 071703.
22. Moharana, M. K., & Khandekar, S. (2013). Effect of aspect ratio of rectangular microchannels on the axial back conduction in its solid substrate. International Journal of Microscale and Nanoscale Thermal and Fluid Transport Phenomena, 4(3-4), 1-19.
23. Yadav, A., Tiwari, N., Moharana, M. K., & Sarangi, S. K. (2014). Axial wall conduction in cryogenic fluid microtube. 5th International and 41st National Conference on Fluid Mechanics and Fluid Power (FMFP-2014) 12-14 December 2014, IIT Kanpur, India.
24. Mishra, P., & Moharana, M. K. (2014, August). Axial Wall Conduction in Pulsating Laminar Flow in a Microtube. In ASME 2014 12th International Conference on Nanochannels, Microchannels, and Minichannels collocated with the ASME 2014 4th Joint US-European Fluids Engineering Division Summer Meeting (pp. V001T02A006-V001T02A006). American Society of Mechanical Engineers.

25. Sawyers, D. R., Sen, M., & Chang, H. C. (1998). Heat transfer enhancement in three-dimensional corrugated channel flow. International Journal of Heat and Mass Transfer, 41(22), 3559-3573.
26. Islamoglu, Y., & Parmaksizoglu, C. (2003). The effect of channel height on the enhanced heat transfer characteristics in a corrugated heat exchanger channel. Applied Thermal Engineering, 23(8), 979-987.
27. Naphon, P. (2009). Effect of wavy plate geometry configurations on the temperature and flow distributions. International Communications in Heat and Mass Transfer, 36(9), 942-946.
28. Sui, Y., Teo, C. J., Lee, P. S., Chew, Y. T., & Shu, C. (2010). Fluid flow and heat transfer in wavy microchannels. International Journal of Heat and Mass Transfer, 53(13), 2760-2772.
29. Abed, W. M., & Ahmed, M. A. (2010). Numerical Study of Laminar Forced Convection Heat Transfer and Fluid Flow Characteristics in a Corrugated Channel. Journal of Engineering and Development, 14(3).
30. Mohammed, H. A., Gunnasegaran, P., & Shuaib, N. H. (2011). Numerical simulation of heat transfer enhancement in wavy microchannel heat sink. International Communications in Heat and Mass Transfer, 38(1), 63-68.
31. Sui, Y., Lee, P. S., & Teo, C. J. (2011). An experimental study of flow friction and heat transfer in wavy microchannels with rectangular cross section. International Journal of Thermal Sciences, 50(12), 2473-2482.
32. Gong, L., Kota, K., Tao, W., & Joshi, Y. (2011). Parametric numerical study of flow and heat transfer in microchannels with wavy walls. Journal of Heat Transfer, 133(5), 051702.

33. Sui, Y., Teo, C. J., & Lee, P. S. (2012). Direct numerical simulation of fluid flow and heat transfer in periodic wavy channels with rectangular cross-sections. International Journal of Heat and Mass Transfer, 55(1), 73-88.
34. Jogi Nikhil G. & Lawankar Shailendra M. Heat Transfer Analysis of Corrugated Plate Heat Exchanger of Different Plate Geometry: A Review. International Journal of Emerging Technology and Advanced Engineering. ISSN 2250-2459, Volume 2.
35. Yin, J., Yang, G., & Li, Y. (2012). The effects of wavy plate phase shift on flow and heat transfer characteristics in corrugated channel. Energy Procedia, 14, 1566-1573.
36. Ozbolat, V., Tokgoz, N., & Sahin, B. Flow Characteristics and Heat Transfer Enhancement in 2D Corrugated Channels.
37. Pehlivan, H., Taymaz, I., & İslamoğlu, Y. (2013). Experimental study of forced convective heat transfer in a different arranged corrugated channel. International Communications in Heat and Mass Transfer, 46, 106-111.
38. Nandi, T. K., & Chattopadhyay, H. (2013). Numerical investigations of simultaneously developing flow in wavy microchannels under pulsating inlet flow condition. International Communications in Heat and Mass Transfer, 47, 27-31.
39. Nandi, T. K., & Chattopadhyay, H. (2014). Numerical investigations of developing flow and heat transfer in raccoon type microchannels under inlet pulsation. International Communications in Heat and Mass Transfer, 56, 37-41.
40. Mishra, P., & Moharana, M. K. (2014), Thermo-Hydrodynamics of Pulsatile Flow in a Microtube: A Numerically Study. Thesis submitted to NIT Rourkela, Mechanical Engineering Department.